CHAPTER 5

The SiO Maser Luminosity...

As a first step towards knowing the relationship between the maser phenomenon and the properties of the Mira variables, in this chapter, we convert the observed maser fluxes into luminosities. To calculate the true maser luminosity, one needs to know or assume something about its isotropy. According to Alcock and Ross (1984), the maser emission is likely to be highly anisotropic. VLBJ observations indicate emission from spots located around the star over a region of angular dimensions about 5 times the stellar radius (hloran et al. 1979, Lane et al. 1984, McIntosh et al. 1989). It is likely that the emission is beamed and that some of these beams are aimed towards us appearing as spots. However, at present there is not enough data (e.g., time-monitoring with VLBI), to conclude anything about the geometry of the total emission from the source. We can do no better than to assume that no matter from which direction one is looking at the Mira variable. one would see more-or-less the same number of masing spots and also that their filling factor is the same for all Miras.

5.1 Distances of the Mira variables

Next, to calculate the maser luminosity, we need to know distances of the Mira variables. We have tried all the known methods to find the distances. The method numbered as 7 below was found to be the moat reliable one. To make the reliability of this method apparent, we give below a short description of the other methods.

These are summarized in Fig. 1. In all the methods discussed, distances are obtained by comparing the observed magnitudes with the absolute magnitudes using,

$$m - M = 5logD - 5 + A(D) \quad (1)$$

where D is the distance in parsecs, m is the apparent magnitude and M is the absolute magnitude, A(D) is the extinction function. This equation is solved iteratively, to obtain the distance. The methods differ in the ways of obtaining the apparent and absolute magnitudes, and the extinction correction.

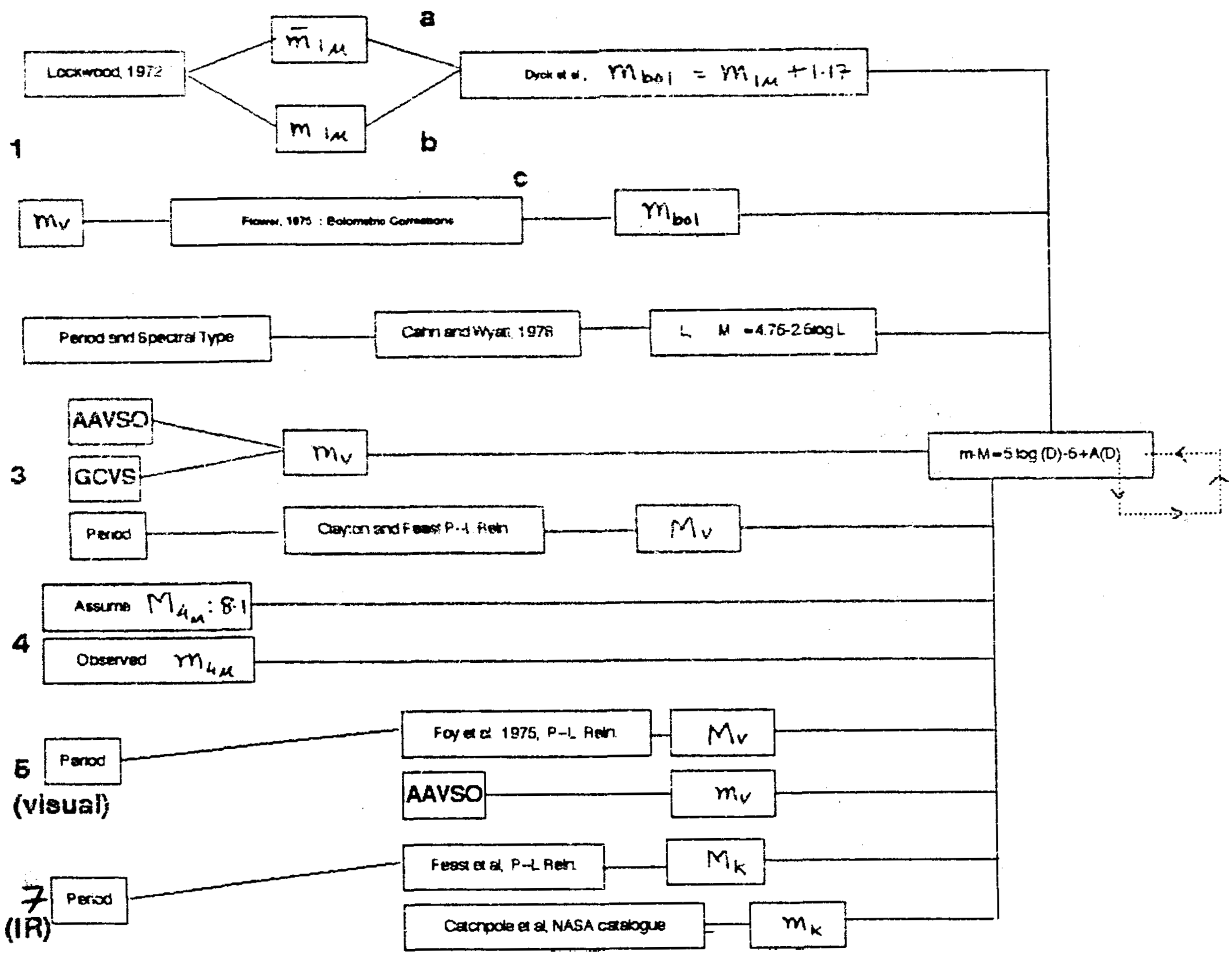

Figure 1: Summary of methods to obtain the distances to Mira variables

1. Cahn and Wyatt 1978.

These authors provide a plot of mass v/s luminosity, with curves of constant periods and constant spectral-types drawn over it (see Fig. 2 of Cahn and Wyatt, 1978). This figure is obtained from a theoretical model of evolution of Mira variables discussed in the paper. Knowing the period and spectral-type of a Mira variable, one can obtain from this figure both, mass and luminosity. Using a constant bolometric correction, they obtain the bolometric magnitude from

$$\overline{M_{bol}} = 4.75 - 2.5 \log L. \qquad (2)$$

The distances quoted in this paper are reproduced in column 1 of Table 1. Distances obtained by the same method applied to some other SiO sources, by Snyder et al. (1978), are listed in column 1. As seen from Fig. 1, there are three observed quantities which can go as inputs to this method. Corresponding to these, we have listed the distances in columns 1a, 1b, and 1c of Table 1. It is interesting to note that there are several well known Mira variables which fall outside the "wedge" in Fig. 2. of Cahn and Wyatt's paper. The authors had claimed that the Mira phase in the star's evolution occured only inside this wedge.

2. Eggen 1971.

This author has used some stars in the Hyades cluster and calibrated the absolute magnitudes against $(R-I)$ colours. This calibration is then used to obtain the absolute magnitudes for other stars, from their $(R-I)$. There is no correction applied for interstellar extinction. These values of distances are listed in column 2 of Table 1.

Table 1: Distances using various methods

No.	SOURCE	Quoted						
		cal.	1	2	3	4	5	6
1	AFGL 3068							
2	AFGL1977							
3	AND W							
4	AND Z							
5	ANT V						1227	
6	AQL MU							
7	AQL RT						637	635
8	AQL V450							
9	AQR EP							
10	AQR R					181		
11	ARI R							
12	ARI U							
13	AUR EY							
14	AUR NV							
15	AUR R							
16	AUR U							
17	AUR UV							
18	AUR YY							
19	BOO R							
20	BOO RX						460	
21	BOO Z							
22	CAE R					440		
23	CAM TX		696		870			
24	CAM W							
25	CAS R		266		322		230	207
26	CAS Y						620	538
27	CEN RT							
28	CEN RX							
29	CEN TU							
30	CEN UU							
31	CEN V423							
32	CEN V744							
33	CEN VX							
34	CEN Y							
35	CEP MU							
36	CEP T		240		233			
37	CET O	76	114		84		77	
38	CMA CY							
39	CMA DN							
40	CMA SY							

Table 1: (contd.)

No.	SOURCE		Quoted					
		cal.	1	2	3	4	5	6
41	CMA VY							
42	CMI S							
43	CMI U							
44	CNC R		339		343			
45	CNC RR							
46	CNC RS							
47	CNC RT							
48	CNC T							
49	CNC W							
50	CNC X							
51	COL W							
52	COM R							
53	CRB S		467		492		397	384
54	CRT R					294	741	
55	CRT S							
56	CRV R							
57	CVN T							
58	CVN TX							
59	CVN V							
60	CYG CHI							
61	CYG KY							
62	CYG R							
63	CYG SX							
64	CYG U							
65	CYG UX						555	1118
66	CYG V407							
67	CYG Z						990	829
68	DOR R						234	
69	DRA R							
70	ERI V							
71	ERI W					580	679	
72	ERI Z			265				
73	GEM EE							
74	GEM UZ							
75	HER RU				575			714
76	HER T							
77	HER U		397		454		322	321
78	HER V443							
79	HOR R						177	
80	HYA R	166		160	124			

Table 1: (contd.)

No.	SOURCE		Quoted					
		cal.	1	2	3	4	5	6
81	HYA RR							
82	HYA RT							
83	HYA RU		734				671	
84	HYA S							
85	HYA SW							
86	HYA T							
87	HYA TU							
88	HYA U							
89	HYA V							
90	HYA W		135					100
91	HYA X						765	
92	HYA Y							
93	IR 11							
94	IR 6							
95	IRC+60169							
96	IRC+70066							
97	IRC-10414							
98	IRC-10529							
99	LEO R	191	147	148	258		238	129
100	LEO S			410				
101	LEO VY							
102	LEP R							
103	LEP RT							
104	LEP SY							
105	LEP T					306		
106	LIB FS							
107	LIB RR							
108	LIB RS							
109	LIB RU							
110	LMI R						352	324
111	LMI RW							
112	LUP R							
113	LYR RW							
114	LYR V							
115	MIC T							
116	MIC V						906	
117	MON ER							
118	MON FX							
119	MON GN							
120	MON GX							

Table 1: (contd.)

No.	SOURCE	Quoted						
		cal.	1	2	3	4	5	6
121	MON U							
122	MON V							
123	OPH R							
124	OPH RS							
125	OPH RT							
126	OPH RU							
127	OPH V1111							
128	ORI DT							
129	ORI EP							
130	ORI EU							
131	ORI S							
132	ORI U				292		239	282
133	ORI V							
134	ORI W							
135	PEG R		499		557		470	420
136	PER AX							
137	PER S							
138	PIC S						322	
139	PSC R							
140	PSC WX							
141	PUP Z							801
142	PYX S							
143	PYX X							
144	SCO AH							
145	SCO RR	275						
146	SER S							
147	SER WX				1785	562	1720	
148	SGE HM							
149	SGR RR						336	476
150	SGR VX							
151	TAU NML		400					
152	TAU R						743	594
153	UMA R							
154	UMA ST							
155	UMA T							
156	UMI RR							
157	UMI S							
158	VEL RW							
159	VIR BK							

Table 1: (contd.)

No.	SOURCE	Quoted						
		cal.	1	**2**	**3**	4	5	6
160	VIR R							
161	VIR RT						1150	
162	VIR RU							
163	VIR S							477
164	VIR SS						330	
165	VIR SW			272				
166	VUL R							
167	SCL S	437						
168	MEN U	437						
169	MON X	347						
170	OPH X	251						

Table 1: (contd.)

No.	SOURCE	Calculated				
		Cla	Clb	Clc	Visual	IR
1	AFGL 3068					
2	AFGL1977					
3	AND W			1091	347	
4	AND Z					
5	ANTV			692	923	
6	AQLMU				2628	
7	AQL RT			644	596	480
8	AQL V450					121
9	AQREP					52
10	AQRR			516	254	424
11	ARI R				798	1377
12	ARI U			1298	354	698
13	AUREY			3494	2219	
14	AURNV					1360
15	AURR	467	460	320	318	255
16	AURU			417	527	495
17	AURUV			391	954	766
18	AURYY			7647	2458	
19	BOOR					667
20	BOO RX			815	767	138
21	BOO Z			1210	1080	1714
22	CAE R			520	459	457
23	CAM TX			1699	929	317
24	CAM W				1969	
25	CAS R	289	233	223	237	164
26	CAS Y			1351	450	586
27	CEN RT				664	920
28	CEN RX			1686	729	1078
29	CEN TU			3080	1108	
30	CEN UU			659	1140	
31	CEN V423				3431	
32	CEN V744				173	142
33	CEN VX			3171	300	356
34	CEN Y				997	181
35	CEP MU					238

Table 1: (contd.

No.	SOURCE	Calculated				
		Cla	Clb	Clc	Visual	IR
36	CEP T	227	254	327	193	178
37	CET O	115		79	82	112
38	CMA CY				3303	423
39	CMA DN					
40	CMA SY			3754	1962	
41	CMA VY					
42	CMI S					401
43	CMI U			2001	443	1097
44	CNC R			359	316	234
45	CNC RR			4323	1500	
46	CNC RS				312	83
47	CNC RT				415	124
48	CNC T				298	655
49	CNC W			532	364	594
50	CNC X				299	262
51	COL W				947	
52	COM R			898	684	980
53	CRB S			309	394	323
54	CRT R				1670	121
55	CRT S				2602	285
56	CRV R			776	482	750
57	CVN T					794
58	CVN TX					
59	CVN V				391	390
60	CYG CHI	22	14		120	762
61	CYG KY	22	64			
62	CYG R				324	827
63	CYG SX					753
64	CYG U				224	736
65	CYG UX					1078
66	CYG V407					
67	CYG Z			683	618	752
68	DOR R					60
69	DRA R					727
70	ERI V				961	114

Table 1: (contd.

No.	SOURCE	Calculated				
		Cla	Clb	Clc	Visual	IR
71	ERI W			384	664	814
72	ERI Z				408	157
73	GEM EE			6411	2412	
74	GEM UZ				2850	
75	HER RU				357	512
76	HERT					1414
77	HERU	533	454	354	364	325
78	HER V443				106	
79	HORR			329	189	575
80	HYA R			116	102	119
81	HYARR			2782	976	1265
82	HYA RT			444	400	294
83	HYA RU			556	673	671
84	HYA S			969	608	1037
85	HYA SW				1630	
86	EIYA T			1074	564	881
87	HYA TU			3484	2082	
88	HYA U				96	293
89	HYA V				129	348
90	HYA W			280	453	92
91	HYA X					408
92	HYA Y				377	346
93	IR 11					
94	IR 6					
95	IRC+60169					
96	IRC+70066					
97	IRC-10414					
98	IRC-10529					
99	LEO R	139	126	143	193	108
100	LEO S				1454	3308
101	LEO VY					
102	LEPR .			508	247	384
103	LEP RT			272	1485	
104	LEP SY			7461	3663	
105	LEP T			664	388	350

Table 1: (contd.

No.	SOURCE	Calculated				
		Cla	Clb	Clc	Visual	IR
106	LIB FS			5826		1275
107	LIB RR			1350	682	1062
108	LIB RS					247
109	LIB RU					902
110	LMI R	358	387	307	344	272
111	LMI RW					778
112	LUP R				1512	939
113	LYR RW			1509	1412	1019
114	LYR V			529	835	888
115	MIC T					169
116	MIC V				947	1043
117	MON ER				5809	
118	MON FX				2986	875
119	MON GN					
120	MON GX			1285	2262	921
121	MON U				289	634
122	MON V					511
123	OPH R					469
124	OPH RS					
125	OPH RT					817
126	OPH RU				1364	1680
127	OPH V1111					
128	ORI DT				2104	962
129	ORI EP				1470	
130	ORI EU			5306	1682	
131	ORI S			507	302	345
132	ORI U	393	347	200	238	231
133	ORI V			2626	1097	1659
134	ORI W				266	221
135	PEG R	513	526	554	460	471
136	PER AX					7558
137	PER S					761
138	PIC S			378	295	548
139	PSC R					916
140	PSC WX					1129

Table 1: (contd.

No.	SOURCE	Calculated				
		Cla	Clb	Clc	Visual	IR
141	PUP Z				343	761
142	PYX S				1052	1372
143	PYX X				4971	2120
144	SCO AH					533
145	SCO RR			174	252	243
146	SER S			871	715	728
147	SER WX			9445	2739	1197
148	SGE HM					
149	SGR RR			509	324	472
150	SGR VX					410
151	TAU NML			4086	2131	262
152	TAU R			1001	700	439
153	UMA R					313
154	UMA ST				341	214
155	UMA T					1018
156	UMI RR					57
157	UMI S					369
158	VEL RW					308
159	VIR BK				550	134
160	VIR R				457	507
161	VIRRT				1208	137
162	VIR RU			414	1076	573
163	VIR S			410	327	416
164	VIR SS			348	312	463
165	VIRSW				455	86
166	VUL R					

3. Cahn 1976.

Column **3** of Table 1, lists the distances obtained from equation **1,** where now the bolometric magnitude is replaced by visual magnitude, M_v, obtained from a period-luminosity relation given by Clayton and Feast (1970). The extinction is calculated from a transformation of the colour excess.

4. Lepine et al. 1978

These authors have assumed that all Mira variables have the same luminosity at the wavelength of 4μ, and its value is -8.1, this value is then compared with the observed flux at 4μ and the distance is again obtained using the same equation (ignoring the extinction). These values of distances are listed in column 4 of Table 1.

5. Lepine arid Paes de Barros (1977).

Column 5 of Table 1, lists distances which are quoted from the above paper, using the following method. The absolute visual magnitude is obtained from an empirical period-luminosity relation given by Foy et al. (1975), which is nearly the sarne as the one referred to earlier (Clayton and Feast, 1970). The discrepancy between the two occurs for stars in the period bin 150–200 days; the value of absolute magnitude as given by Clayton and Feast is **-3,** while it is -1.75 magnitudes according to Foy et al. The reason for this discrepancy is discussed by Robertson and Feast(1981). They favour the P-L relation of Clayton and Feast which is in agreement with that obtained from the globular cluster Miras. The advantage of using the visual magnitude is that it is a well observed quantity for a very large number of stars, unlike the infrared magnitude. The disadvantage lies in its sensitivity to the interstellar extinction correction. In this method the extinction correction is estimated from the following formula, (Sharov, 1964)

$$A(D, b) = \frac{a_o \beta}{sin(b)} \left(1 - \exp \frac{-D sin(b)}{P}\right), \qquad (3)$$

where the mean values of the constants a_o and β are quoted as 0.1824 magnitudes and 114 parsecs, respectively.

6. The distances quoted in column 6 of Table 1, are also from the same reference. But they are derived using a different method, which assumes the infra-red magnitude at 1 micron to be independent of period and equal to -6.5. The apparent magnitude is obtained from observations of Lockwood (1972). The extinction correction at this wavelength is assumed to be half of the value given by equation **3.**

7. Mira variables are intrinsically very luminous objects arid their brightness peaks at infrared wavelengths. Observations of these objects at IR wavelengths, for determining distances has the advantage that the problem of interstellar extinction is less severe. The first attempt in this direction was made by Robertson and Feast (1981). They calibrated the absolute bolometric magnitudes of galactic Mira variables using both statistical parallaxes (following Clayton and Feast 1969), and the distances to a small number of individual variables. The column with the heading 'cal.' in Table 1, lists these stars seperately for comparison of their distances obtained by various methods. Subsequently, Glass and Lyodd-Evans (1981) showed that Mira variables in the LMC satisfy a well defined P-L relation with very little scatter. Menzias and Whitelock (1985) and Feast (1984), find that the galactic cluster Miras also follow a P-L relation whose slope and zero-point are not significantly different from that of the LMC Miras

(Feast,1986). This universal P-L relation is given by,

$$M_{bol} = 1.12 - 2.432 \log \mathrm{P}. \tag{4}$$

The uncertainty in M_{bol} is about 0.1 magnitude, within which there is no evidence at present, of the alleged effect of different metal abundances on the zero-point of the P-L relation (Feast, 1986). While the M_{bol}—P-L relation is also important for theoretical studies (e.g., H-R diagram, nature of pulsation — whether Miras are fundamental or overtone pulsators...), for practical applications like distance determination, it is useful to have a similar period-luminosity relation at some infra-red wavelengths at which there exist a large number of photometric observations. Glass and Feast (1982) find such relations for the J, H and K bands, for some Miras in the LMC. All these relations (including the bolometric), have the same order of uncertainties (0.1—0.2 magnitudes), within which they agree with each other. Later, Feast (1984) made a comparative study of the zero-points and slopes of the various P-L relation for the LMC as well as the galactic Miras and concluded that currently, the best available period-luminosity relation for Mira variables is in terms of the K-magnitudes, and is given by,

$$M_K = 0.53 - 3.291 \log \mathrm{P}, \tag{5}$$

with a a of about 0.1 magnitude. We have used this relation to derive the distances to the Mira variables in our sample. We have corrected the apparent magnitudes for interstellar extinction according to Feast et al. (1982),

$$A_K = \frac{0.12}{\sin \mathrm{b}} \left(1 - e^{-10r \sin(b)}\right), \tag{6}$$

where r is the distance in kpc and b is the galactic latitude. The apparent K magnitudes were obtained from Catchpole et al. (1979) and from NASA IR-catalogue (1984). The distances obtained by this method, are listed in Table 2 . Both these distances are compared with the calibrator distances in Fig. 2. From it, the agreement between these methods seems to be good. But in Fig. 3, which compares distances obtained by the two methods, we see that there are a substantial number of objects for which the visual method gives a significantly different distance compared to the infra-red method. This discrepancy may be due to poor extinction correction and to a smaller extent, an error in the infra-red P-L relation. We feel that the IR distances are more reliable due to their relative insensitivity* to extinction corrections. We therefore have adopted these distances.

The distances are expected to be independent of the intrinsic stellar characteristics. As a check, we have plotted the adopted IR distances against the amplitude of pulsation in visual magnitude in Fig. 4., and against other stellar quantities, in Figs 5 – 7. Fig. 4 shows that the scatter is almost uniform, except in the small range of amplitudes around 5 magnitudes. The selection of sources in our sample was without any regard to their visual amplitude. However, the histogram of visual amplitude for the galactic Miras (from the General Catalogue of Variable Stars), peaks approximately in this range (Ikaunieks 1975), therefore, in a randomly drawn sample we would expect a similar distribution which is roughly consistent with a slight excess of scatter in the amplitude bin 4 to 6 magnitudes, in Fig. 4. However, we note that given a distribution of Mira variables in the Galaxy with no preferred spatial location for a particular intrinsic

* We estimate an error in these to be about 20% which is mainly due to the error in distance modulus.

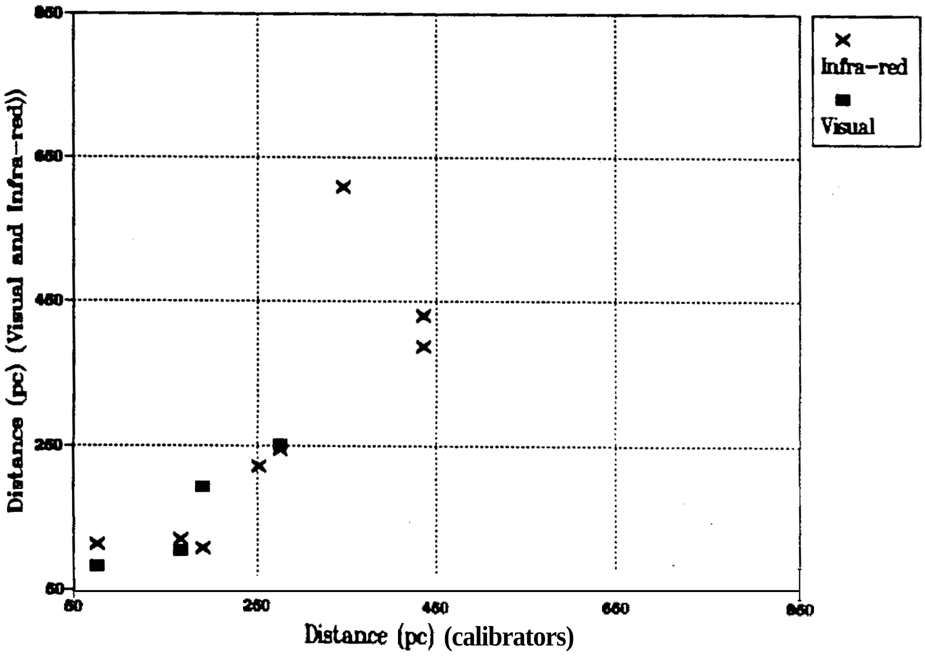

Figure 2: Comparison of the visual and IR distances with the Calibrator distances

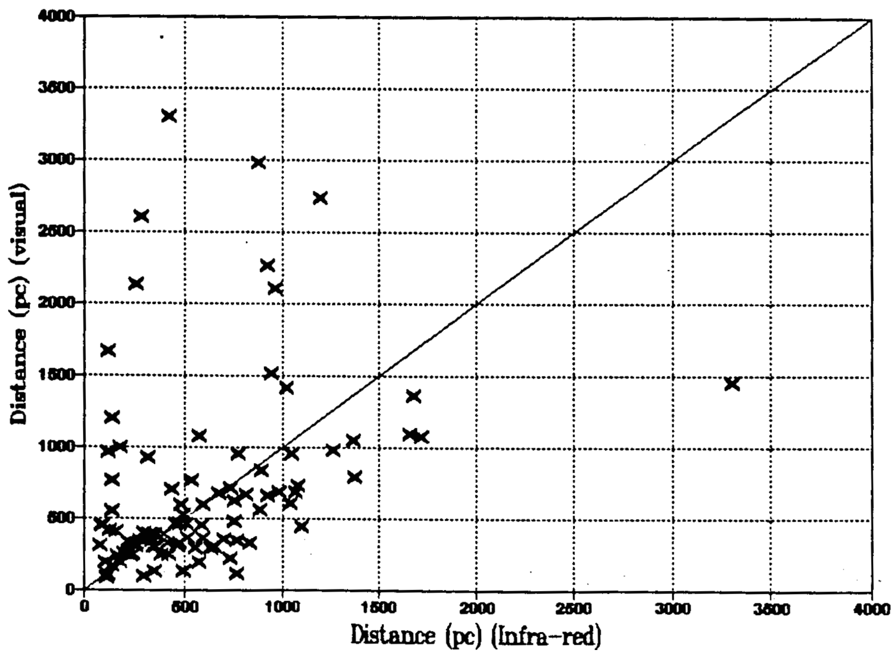

Figure 3: Comparison of the visual distances with the IR distances

stellar characteristic, one would expect a larger number of Mira variables for greater distances, regardless of the value of any intrinsic stellar quantity. This does not seem to hold in Figs 4 – 7. This descrepancy could be due to an inadequate extinction correction.

5.2 The maser luminosity

As discussed earlier, we have determined the distances to the Mira variables in our sample and obtained the maser luminosities from the observed integrated fluxes under the spectral-lines, by assuming isotropic emission. The photon luminosity of the maser is then given by,

$$L = \frac{s_\nu}{h\nu} 4\pi D^2, \tag{7}$$

where s_ν is the integrated flux in Jy km s^{-1}, and D is the distance in parsecs.

These distances and luminosities are listed in Table 2. In the next chapter, we compare the maser luminosity with some intrinsic property of Mira variables.

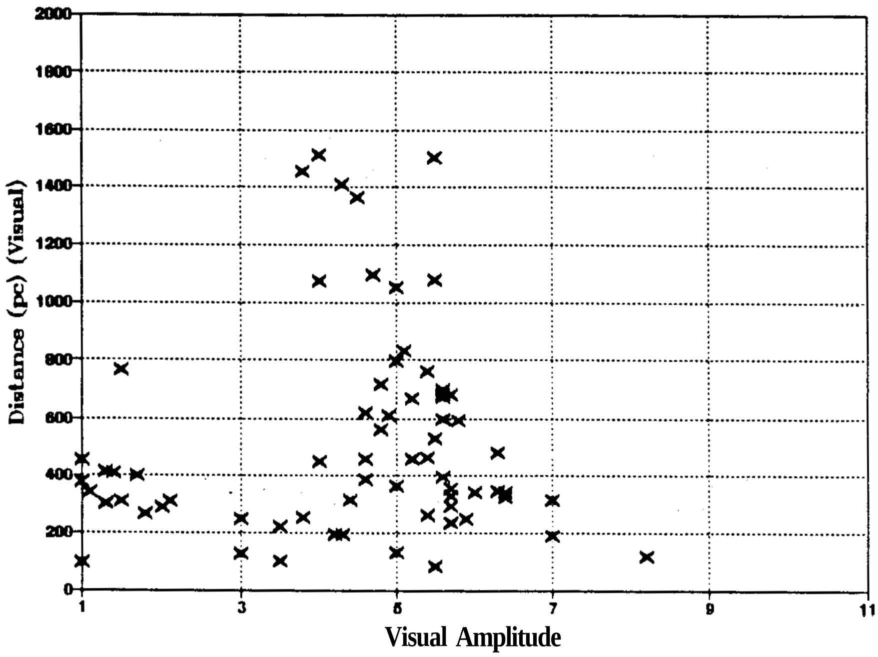

Figure 4: Checking for a correlation between the distance and the visual amplitude

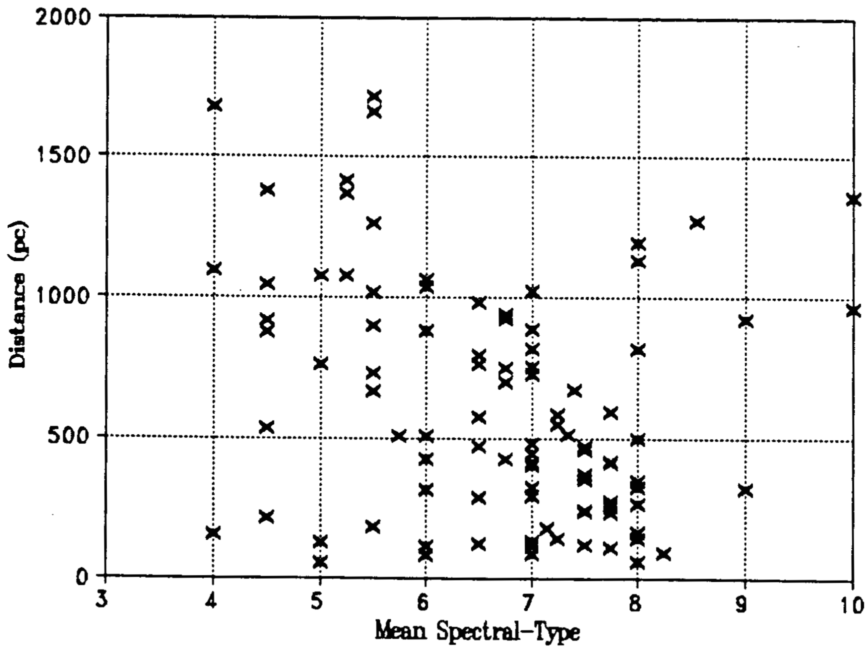

Figure 5: Checking for a correlation between the distance and the mean spectral-type

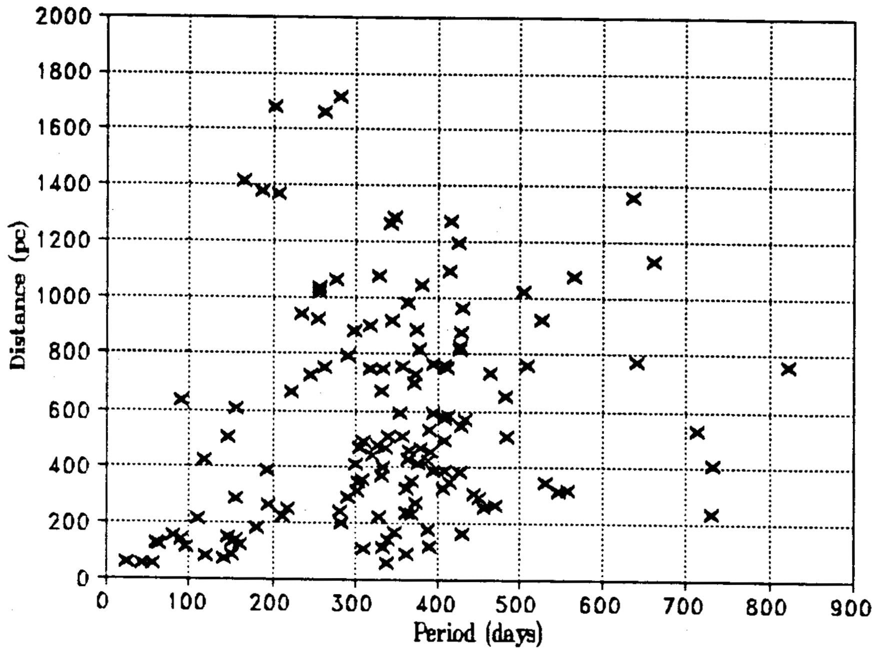

Figure 6: Checking for a correlation between the distance and the period

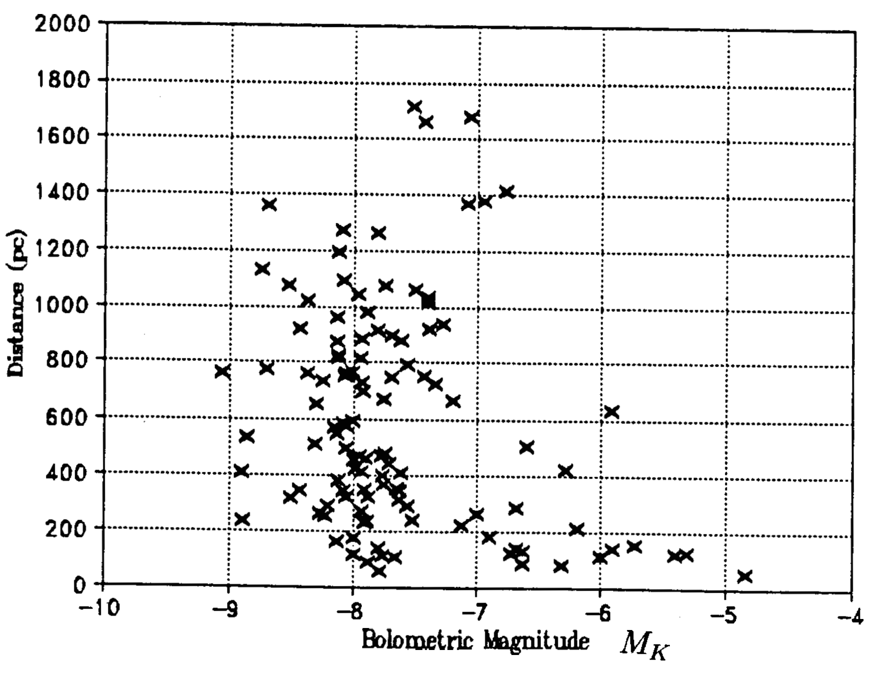

Figure 7: Checking for a correlation between the distance and the bolometric-magnitude

Table 2. Distances and Luminosities

No.	Source	Distance (pc)	SiO Lum. phot./s	No.	Source (pc)	Distance phot./s	SiO Lum.
1	AQL RT	480	< 0.07	31	CRT R	121	0.03
2	AQR R	424	0.45	32	CRT S	285	< 0.03
3	ARI R	1377	< 0.87	33	CRV R	750	< 0.21
4	ARI U	698	< 0.21	34	CYG CHI	762	5.92
5	AUR R	255	< 0.03	35	CYG R	827	< 0.40
6	AUR U	495	< 0.09	36	CYG U	736	< 0.28
7	AUR UV	766	< 0.22	37	CYG UX	1078	< 1.96
8	BOO RX	138	0.02	38	CYG Z	752	< 0.29
9	BOO Z	1714	< 1.08	39	ERI V	114	< 0.01
10	CAE R	457	0.39	40	ERI W	814	< 0.30
11	CAM TX	317	0.57	41	ERI Z	157	< 0.01
12	CAS R	164	0.08	42	HER RU	512	< 0.12
13	CAS Y	586	< 0.16	43	HER U	325	0.49
14	CEN RT	920	< 0.50	44	HOR R	575	0.54
15	CEN RX	1078	< 0.34	45	HYA R	119	0.05
16	CEN V744	142	< 0.01	46	HYA RR	1265	< 0.35
17	CEN VX	356	< 0.08	47	HYA RT	294	< 0.04
18	CEN Y	181	< 0.01	48	HYA RU	671	0.31
19	CEP T	178	< 0.02	49	HYA S	1037	< 0.55
20	CET O	112	0.81	50	HYA T	881	< 0.28
21	CMA CY	423	< 0.08	51	HYA U	293	< 0.03
22	CMI U	1097	< 0.53	52	HYA V	348	< 0.04
23	CNC R	234	0.23	53	HYA W	92	0.52
24	CNC RS	83	< 0.01	54	HYA Y	346	< 0.05
25	CNC RT	124	< 0.01	55	LEO R	108	0.25
26	CNC T	655	0.20	56	LEO S	3308	< 4.82
27	CNC W	594	< 0.13	57	LEP R	384	< 0.07
28	CNC X	262	< 0.03	58	LEP T	350	< 0.04
29	COM R	980	< 0.35	59	LIB FS	1275	< 0.48
30	CRB S	323	0.24	60	LIB RR	1062	< 0.41

Table 2. (contd.)

No.	Source	Dist.(pc) (pc)	SiO Lum. phot./s	No.	Source (pc)	Distance phot./s	SiO Lum.
61	LMI R	272	0.14	79	PYXS	1372	< 1.10
62	LUP R	939	< 0.65	80	PYX X	2120	< 2.31
63	LYR RW	1019	< 0.38	81	SCO AH	533	0.81
64	LYR V	888	< 0.58	82	SCO RR	243	< 0.02
65	MIC V	1043	< 0.72	83	SER S	728	< 0.39
66	MON FX	875	< 0.34	84	SER WX	1197	< 1.05
67	MON GX	921	1.06	85	SGR RR	472	< 0.10
68	MON U	634	< 0.12	86	SGR VX	410	4.38
69	OPH RU	1680	< 1.03	87	TAU NML	262	0.59
70	ORI DT	962	< 0.68	88	TAU R	439	< 0.09
71	ORI S	345	< 0.04	89	UMA ST	214	< 0.01
72	ORI U	231	0.20	90	VIR BK	134	< 0.01
73	ORI V	1659	< 1.21	91	VIR R	507	< 0.09
74	ORI W	221	< 0.02	92	VIR RT	137	0.02
75	PEG R	471	0.69	93	VIR RU	573	< 0.07
76	PER S	761	1.91	94	VIR S	416	< 0.10
77	PIC S	548	< 0.25	95	VIR SS	463	< 0.10
78	PUP Z	761	0.70	96	VIRSW	86	0.02

Table 2. (1990 sources) (contd.)

No.	Source	Distance (pc)	SiO Lum. phot./s
1	AQL RT	480	< 0.21
2	AQL V450	121	< 0.01
3	AURNV	1360	2.07
4	AUR R	255	< 0.07
5	BOO R	667	< 0.44
6	CEP MU	238	0.49
7	CMI S	401	< 0.13
8	CVN T	794	< 0.45
9	CYGSX	753	< 0.56
10	DORR	60	0.05
11	DRA R	727	< 0.37
12	HERT	1414	< 1.86
13	HYA X	408	< 0.11
14	LEP T	350	< 0.14
15	LIB RU	902	< 0.88
16	LMI RW	778	< 0.35
17	LYRV	888	< 0.57
18	OPH RT	817	< 0.59
19	PIC S	548	< 0.35
20	PSC R	916	< 1.02
21	PSC WX	1129	2.71
22	SCO RR	243	< 0.04
23	SGR RR	472	< 0.22
24	UMAR	313	< 0.07
25	UMAT	1018	< 0.75
26	UMI RR	57	< 0.01
27	UMI S	369	< 0.14
28	VIR R	507	< 0.22
29	VIR S	416	0.21
30	VIR SS	463	< 0.17

REFERENCES

Alcock C., Ross R. R., 1986, *Ap.* **J.** 310,838.

Cahn J.H., 1976, *Ap.* **J.** 81,407.

Cahn J. H., Wyatt S. P., 1978, **A,.** **J.** 221.163.

Catchpole R. M. et al. 1979, *South African Astronomical Observatory Circulars* **1**,61.

Clayton M. L., Feast M. W., 1970, *Mon. Not. Royal Astron. Soc.* 146,411.

Eggen O. J., 1971, **Ap. J.** 165,317.

Feast M. W., 1982, *Mon. Not. Royal Astron. Soc.* 201,439.

Feast *M*. W., 1984, *Mon. Not. Royal Astron. Soc.* **211**,51p.

Feast M. W., 1986, *"Light on Dark Matter"*, 1st IRAS Conf. Proc., Ed.: Israel F. P., (D. Reidel Publ. Co.)

Foy R., Heck A., Mennessier M. O., 1975, *Astron. Astrophys.* 43,175.

Kholopov P. N. et al. (Ed.), 1985, General Catalogue of Variable Stars, (hloscow Publishing House).

Glass I. S., Feast M. W., 1982, *Mon. Not. Royal Astron. Soc.* 198,199.

Class I. S., Lyodd-Evans T., 1981, *Naturc* 291,303.

Keenan P. C., Garrison R. F., Deutsch .4. J., 1974, *Ap.* **J.** *Suppl. Ser.* 28,271.

Ikaunieks J., 1975, *Pulsating Stars* Ed. Kukarkin B. V. (John Wiley and Sons.) p 259.

Lane A. P., 1984, IAU Symp 110, VLBI and compact radio sources, p 329, (D. Reidel Publ. Co.)

Lepine J. R. D., Paes de Barros M. H., 1977, *Astron. Astrophys.* 56,219

Lepine J. R. D., LeSqueren A. M., Scalise E. Jr., 1978, *Ap.* **J.** 225,869.

Lockwood G. R., 1972, *Ap.* **J.** *Suppl. Ser.* 24,375.

McIntosh G. C.,et al. 1989, *Ap.* **J.** 337,934.

Menzias J. W., Whitelock P. A., 1985, *Mon. Not. Royal Astron. Soc.* 212,783.

Gezari D. Y., Schmitz M., Mead J. M., 1984, *Catalog of Infrared Observations,* NASA Ref. Publ. 1118.

Moran J. M., et al. 1979, *Ap.* **J.** 231,124.

Pettit E., Nicholson S. B., 1933, *Ap.* **J.** 78,320.

Robertson B. S. C., Feast M. W., 1981 *Mon. Not. Royal Astron. Soc.* 196,111.

Sharov A. S., 1964, *Soviet Astronomy* 7,689.

Snyder L. E., et al. 1978, *Ap.* **J.** 224,514.

Do all Mira variables show the SiO maser emission? In this chapter we shall address this question, with an emphasis on the spectral-type of the Mira variable and its evolutionary status. Preliminary attempts at studying the correlation of the maser power with spectral-type were made by Cahn (1977) and Spencer et al. (1977). Although their investigations were not conclusive enough, this topic has not been followed up since then.

Cahn (1977) reports a correlation between the absolute maser luminosity and the spectral-type. The conclusion he drew from this correlation is that for every spectral-type, there is a maximum value of maser power which the Mira variable attains on approaching the pulsational phase corresponding to the maximum light. Then, by knowing the spectral-type and the optical phase of the star, one could predict its maser power, and use its observation to obtain the distance to the Mira variable. The range of spectral-types covered by Cahn is from M6 to M10, and observations of 15 sources were considered in his study. No negative detections were included. Subsequently, Dickinson et al. (1978). found seven new Mira variables to be masing, and noted that all had spectral-types later than M4. Of these, Y Cas fitted in the above mentioned correlation while RT Aql did not. The dependence of maser luminosity on spectral-type earlier than M6 not considered by Cahn, remained uninvestigated even later due to lack of adequate observations.

Spencer et al. (1977) noted that at spectral-types near M8, the probability for a Mira variable to show SiO maser emission is greater than 40%. Their sample consisted of 81 stars with very few objects earlier than M6. Their detection limit was **30** Jy and their conclusions were based on fluxes, without taking distances into account.